

**Simulations of Dyon Configurations
in $SU(2)$ Yang-Mills theory**

BACHELORARBEIT

zur Erlangung des akademischen Grades
B.Sc. im Fach Physik

eingereicht von
Benjamin Frank Maier

geboren am
24. Dezember 1988 in Berlin

Betreuer: 1. Prof. Dr. M. Müller-Preußker
 2. Dr. M. Wagner

eingereicht am: 22. August 2011

Abstract

In this work, I investigate several aspects to analyze dyons as generators of confinement. These particles are described within in the semiclassical approach for solving the $SU(2)$ Yang-Mills field equations at finite temperature. At first, analytical expressions for non-interacting dyon configurations are evaluated numerically to obtain the Polyakov loop correlator and consequently the free energy for a static quark antiquark pair in finite and infinite volume. Here, a linear behavior for growing quark separation and therefore confinement is observed. Afterwards, I study a numerical approach called “Ewald’s method”, which efficiently allows to evaluate the gauge potential of a superposition of dyons numerically, which is necessary to calculate the Polyakov loop correlator. The results obtained with this method are in agreement with the analytical results, but the method has the advantage that it can also be applied to interacting dyons. In the last part, I propose a method to treat dyon ensembles with interactions and outline a Metropolis algorithm for generating dyon configurations again using Ewald’s method.

Zusammenfassung

In dieser Arbeit verwende ich verschiedene Methoden, um Dyonen als Erzeuger von Confinement zu untersuchen. Hierbei sind Dyonen Teilchen aus einem semiklassischen Zugang zur Lösung der $SU(2)$ Yang-Mills Feldgleichungen bei endlicher Temperatur. Zuerst werden analytische Ausdrücke für nichtwechselwirkende Dyonen numerisch ausgewertet, um den Polyakov-Loop-Korrelator zu berechnen und folglich die Freie Energie für ein statisches Quark-Antiquark-Paar zu erhalten. Für diese wird ein lineares Verhalten bei steigendem Quarkabstand und damit Confinement beobachtet. Anschließend untersuche ich die sogenannte Ewaldsummation, eine Methode, mit der das Eichpotential einer Superposition von Dyonen numerisch effizient berechnet werden kann, was notwendig für die Auswertung des Polyakov-Loop-Korrelators ist. Die Ergebnisse zeigen Übereinstimmung mit den analytischen Resultaten, allerdings hat diese Methode den Vorteil, auch für wechselwirkende Dyonen Berechnungen zu ermöglichen. Im letzten Teil der Arbeit schlage ich eine Methode vor, wechselwirkende Dyonen zu untersuchen und beschreibe mithilfe der Ewaldsummation einen Metropolisalgorithmus, um für diesen Fall Dyonkonfigurationen zu erzeugen.

Contents

1	Introduction	1
1.1	Relevant Formulae for the Dyon Model	2
2	Semi-Analytical Calculation of the Free Energy for Non-Interacting Dyons	5
2.1	Problem Statement	5
2.2	Evaluation of f_{\pm}	6
2.3	Extrapolation to Infinite Volume	8
2.4	Numerical Results	9
3	Ewald Summation	11
3.1	Introduction	11
3.2	Derivation of Relevant Formulae	12
3.3	Detailed Description of the Algorithm	15
3.3.1	Computational Cost	15
3.3.2	Technical Aspects	15
3.4	Numerical Results for Dyon Ensembles	17
4	Computing the Effective Action of Interacting Dyons	19
4.1	Effective Action	19
4.2	Periodicity	20
4.3	Logarithmic Behavior for Small Separations	22
4.4	Metropolis Algorithm	24
5	Summary and Outlook	27

Chapter 1

Introduction

This work is based on pure $SU(2)$ Yang-Mills theory, which is a crude approximation of Quantum Chromodynamics (QCD), where only two instead of three color charges exist. Furthermore, there are no dynamical quarks, therefore gluon fields are the only degrees of freedom. Studying this theory, one hopes to understand certain aspects of QCD, e.g. “confinement”. This term denotes the phenomenon, that isolated quarks have never been observed in experiments, but only quarks in bound states.

An approach particularly useful to obtain a qualitative understanding of certain phenomena of Yang-Mills theory is semi-classical approximation. In this method, one expands the path integral around classical solutions of the Yang-Mills field equations, where the action is locally minimized. A specific kind of a semi-classical model and its capability to generate confinement is discussed in this work, where the model is based on particles called dyons. These carry electric charge as well as magnetic charge and were first proposed in [1]. Transforming field coordinates to dyon collective coordinates and quantum fluctuations, a Jacobian in the path integral emerges. Part of this Jacobian is the determinant of the so-called “moduli space metric”, which appears as weight factor in the path integral. This was done analytically for calorons [2], whose constituents are a pair of two different-kind dyons. Furthermore, a proposal for a metric of two same-kind dyons was done in [3].

An observable of major interest in this model is the free energy between a static quark antiquark pair, which can be evaluated using the correlation function of the Polyakov loop. In this thesis, I study certain aspects of how to obtain this observable in dyon models with different interactions, organized as follows.

At first, I will give a short description of the relevant formulae for the dyon model and the path integral approach used in this work.

In the second chapter, I will refer to a model of non-interacting dyons, where the moduli space metric equals identity. As shown in [4], one is able to treat this case analytically. I evaluate the necessary expressions for the Polyakov loop correlator numerically and investigate the behavior of the free energy, which turns out to be linear with respect to growing quark antiquark separation, a strong indicator for the generation of confinement.

Afterwards, I introduce a method called “Ewald summation”, which allows to calculate numerically the gauge potential of a superposition of dyons by means of periodic boundary conditions, with a good control of finite size effects, where the gauge potential is necessary

to calculate the Polyakov loop. The results obtained with this method are in agreement with the analytical results. However, this method is more powerful, since it allows to obtain results for interacting dyons, as well.

In chapter four, I will explain a certain way to approximate the interaction of n_D dyons by two-body interactions, first proposed in [5, 6]. Furthermore, I will describe how to obtain an “effective action” by means of Ewald’s method, which makes Monte Carlo simulations with interacting dyons feasible.

1.1 Relevant Formulae for the Dyon Model

The following summary of relevant expressions is adopted from [4]. For a more detailed presentation, I refer to this publication.

Dyons are particles of electric and magnetic charge. A single dyon is associated with a vector potential $a_\mu, \mu \in \{0, 1, 2, 3\}$. However, for this work, the only relevant component of the gauge potential is the Coulomb-like zero-component

$$a_0(\mathbf{r}) = \frac{q}{r},$$

where \mathbf{r} is the spatial distance to the center of the dyon. Here, the charge $q = \pm 1$ denotes two different kinds of dyons. Interactions between two dyons depend on the product of their charge.

The most relevant observable for this work is the Polyakov loop

$$P(\mathbf{r}) = \cos \left(2\pi\omega + \frac{1}{2T} \Phi(\mathbf{r}) \right) \quad (1.1)$$

with the temperature T , the gauge potential of a superposition of dyons

$$\Phi(\mathbf{r}) = \sum_{i=1}^{n_D} a_0(\mathbf{r}_i - \mathbf{r}) = \sum_{i=1}^{n_D} \frac{q_i}{|\mathbf{r}_i - \mathbf{r}|} \quad (1.2)$$

and the holonomy ω . I exclusively concentrate on the maximally non-trivial holonomy $\omega = 1/4$, yielding the Polyakov loop

$$P(\mathbf{r}) = -\sin \left(\frac{1}{2T} \Phi(\mathbf{r}) \right). \quad (1.3)$$

The free energy $F_{Q\bar{Q}}(d)$ between a static quark antiquark pair is given as

$$F_{Q\bar{Q}}(d) = -T \ln \langle P(\mathbf{r})P(\mathbf{r}') \rangle, \quad d = |\mathbf{r} - \mathbf{r}'|, \quad (1.4)$$

with $\langle P(\mathbf{r})P(\mathbf{r}') \rangle$ being the correlation function of Polyakov loops.

For a dyon configuration of n_D dyons at positions $\{\mathbf{r}_k\}$, an expectation value of an observable O is obtained via “path integral”

$$\langle O \rangle = \frac{1}{Z} \int \prod_{i=1}^{n_D} d^3\mathbf{r}_i O(\{\mathbf{r}_k\}) \det G \quad (1.5)$$

$$Z = \int \prod_{i=1}^{n_D} d^3\mathbf{r}_i \det G, \quad (1.6)$$

with G being the moduli space metric describing dyon interactions. This metric depends on the kind of interaction between the dyons and therefore is specified in the corresponding chapters.

Chapter 2

Semi-Analytical Calculation of the Free Energy for Non-Interacting Dyons

2.1 Problem Statement

A non-interacting dyon model was proposed in [4]. Here, the metric for the path integration equals $\text{diag}(1)$, therefore the model can be solved analytically for certain observables. Within this model, n_D dyons are located at random positions in a volume V and the number of positive charged dyons equals the number of negative charged dyons. Using this setup, the correlator of the Polyakov loop Eq. (1.3) can be rewritten (as done in [4]) and finally be evaluated according to

$$\langle P(\mathbf{r})P(\mathbf{r}') \rangle = \frac{1}{2} \exp\left(n_D \ln \frac{|f_-|}{V}\right) - \frac{1}{2} \exp\left(n_D \ln \frac{|f_+|}{V}\right), \quad (2.1)$$

with the integrals

$$f_{\pm} = \int_V d^3s \exp\left(i \frac{1}{2T} \left(\frac{1}{|\mathbf{s} - \mathbf{r}|} \pm \frac{1}{|\mathbf{s} - \mathbf{r}'|} \right)\right). \quad (2.2)$$

These can be computed numerically using Monte Carlo integration. However, the integrals tend to diverge for growing volume. Therefore, in the following, I will show how to rewrite them to make a numerical treatment possible.

Without loss of generality one sets $\mathbf{r} = (0, 0, d/2)$ and $\mathbf{r}' = (0, 0, -d/2)$ and treats $V = \frac{4\pi}{3}R^3$ as a sphere which allows to reduce Eq. (2.2) to a two dimensional integral

$$f_{\pm} = 2\pi \int_0^R ds s^2 \int_0^{\pi} d\theta \sin \theta \exp\left(i \frac{1}{2T} \left(\frac{1}{\sqrt{s^2 - sd \cos \theta + d^2/4}} \pm \frac{1}{\sqrt{s^2 + sd \cos \theta + d^2/4}} \right)\right). \quad (2.3)$$

2.2 Evaluation of f_{\pm}

Evaluation of f_{-}

$\text{Im}(f_{-})$

The integration over θ for the imaginary part of f_{-} can be rewritten according to

$$\text{Im}(f_{-}) \propto \int_0^{\pi} d\theta \sin \theta \sin \left[\frac{1/2T}{\sqrt{s^2 + d^2/4 - ds \cos \theta}} - \frac{1/2T}{\sqrt{s^2 + d^2/4 + ds \cos \theta}} \right] \quad (2.4)$$

$$\propto \int_{-\pi/2}^{\pi/2} d\theta \cos \theta \sin \left[\frac{1/2T}{\sqrt{s^2 + d^2/4 - ds \sin \theta}} - \frac{1/2T}{\sqrt{s^2 + d^2/4 + ds \sin \theta}} \right]. \quad (2.5)$$

Since the integrand is an odd function and the integration is done over a symmetric interval, $\text{Im}(f_{-})$ vanishes.

Proper definition for numerical treatment

At first, the integral is split in two regions, one over a sphere S with radius \tilde{R} and the other one over a hollow sphere $\bar{S} = V \setminus S$:

$$f_{-} = I_{-,1} + I_{-,2}^* \quad (2.6)$$

$$I_{-,1} = 2\pi \int_0^{\tilde{R}} ds s^2 \int_0^{\pi} d\theta \sin \theta \cos \left(\frac{1}{2T} \left(\frac{1}{\sqrt{s^2 - sd \cos \theta + d^2/4}} - \frac{1}{\sqrt{s^2 + sd \cos \theta + d^2/4}} \right) \right), \quad (2.7)$$

$$I_{-,2}^* = 2\pi \int_{\tilde{R}}^R ds s^2 \int_0^{\pi} d\theta \sin \theta \cos \left(\frac{1}{2T} \left(\frac{1}{\sqrt{s^2 - sd \cos \theta + d^2/4}} - \frac{1}{\sqrt{s^2 + sd \cos \theta + d^2/4}} \right) \right). \quad (2.8)$$

The integral $I_{-,1}$ can be computed numerically without any problems. However, $I_{-,2}^*$ tends to diverge for the limit $V \rightarrow \infty$. Therefore one performs an expansion of the integrand in powers of $1/s$ resulting in $(1 + \mathcal{O}((1/s)^4))$. Multiplied with the Jacobian s^2 and integrated over \bar{S} , the diverging part of the integration function is the term 1, which integrates to the volume of the hollow sphere $V(\bar{S}) = V - V(S)$:

$$I_{-,2}^* = 2\pi \int_{\tilde{R}}^R ds s^2 \int_0^{\pi} d\theta \sin \theta + 2\pi \int_{\tilde{R}}^R ds s^2 \int_0^{\pi} d\theta \sin \theta \left[\cos \left(\frac{1}{2T} \left(\frac{1}{\sqrt{s^2 - sd \cos \theta + d^2/4}} - \frac{1}{\sqrt{s^2 + sd \cos \theta + d^2/4}} \right) \right) - 1 \right] \quad (2.9)$$

$$= V(\bar{S}) + I_{-,2}, \quad (2.10)$$

Now $I_{-,2}$ is finite but still not in a proper form for a numerical treatment in the limit $V \rightarrow \infty$, because the upper integration limit is infinity. Hence, one changes variables

according to

$$ds \frac{1}{s^2} = dx, \quad (2.11)$$

leading to $x = -\frac{1}{s} + \frac{1}{\tilde{R}}$. This particular form was chosen because the integrand is proportional to $1/s^2$, thus, it is now approximately equally distributed over the range of integration. Hence, $I_{-,2}$ can be computed in a straight forward way and also rather efficiently.

$$I_{-,2} = 2\pi \int_0^{\frac{1}{\tilde{R}} - \frac{1}{R}} dx s^4 \int_0^{\pi} d\theta \sin \theta \left[\cos \left(\frac{1}{2T} \left(\frac{1}{\sqrt{s^2 - sd \cos \theta + d^2/4}} - \frac{1}{\sqrt{s^2 + sd \cos \theta + d^2/4}} \right) \right) - 1 \right] \quad (2.12)$$

The final result is

$$f_- = I_{-,1} + I_{-,2} + V - V(S). \quad (2.13)$$

Evaluation of f_+

f_+ can be evaluated in an analogous way to f_- by splitting the integral in two regions, where the first integral $I_{+,1}$ can be computed without any problems.

$$I_{+,1} = 2\pi \int_0^{\tilde{R}} ds s^2 \int_0^{\pi} d\theta \sin \theta \exp \left(i \frac{1}{2T} \left(\frac{1}{\sqrt{s^2 - sd \cos \theta + d^2/4}} + \frac{1}{\sqrt{s^2 + sd \cos \theta + d^2/4}} \right) \right) \quad (2.14)$$

Again, the second integral tends to diverge in case of rather large volumes V . Therefore one performs an expansion and subtracts the parts which lead to infinities, arriving at $I_{+,2}$. The divergencies $\Lambda + V(\tilde{S})$ can be obtained analytically, arriving at

$$I_{+,2} = 2\pi \int_0^{\frac{1}{\tilde{R}} - \frac{1}{R}} dx s^4 \int_0^{\pi} d\theta \sin \theta \left[\exp \left(i \frac{1}{2T} \left(\frac{1}{\sqrt{s^2 - sd \cos \theta + d^2/4}} + \frac{1}{\sqrt{s^2 + sd \cos \theta + d^2/4}} \right) \right) \right. \quad (2.15)$$

$$\left. - 1 - \frac{i}{Ts} + \frac{1}{2T^2 s^2} - \frac{i(-3d^2 T^2 + 9d^2 T^2 \cos^2 \theta - 4)}{24T^3 s^3} \right] \quad (2.16)$$

$$\Lambda = 2\pi \int_{\tilde{R}}^R \int_0^{\pi} s^2 ds d\theta \sin \theta \left(\frac{i}{Ts} - \frac{1}{2T^2 s^2} + \frac{i(-3d^2 T^2 + 9d^2 T^2 \cos^2 \theta - 4)}{24T^3 s^3} \right) \quad (2.17)$$

$$= \frac{2\pi}{3T^3} \left(3T(\tilde{R} - R) + 3iT^2(R^2 - \tilde{R}^2) + i \ln \left(\frac{\tilde{R}}{R} \right) \right). \quad (2.18)$$

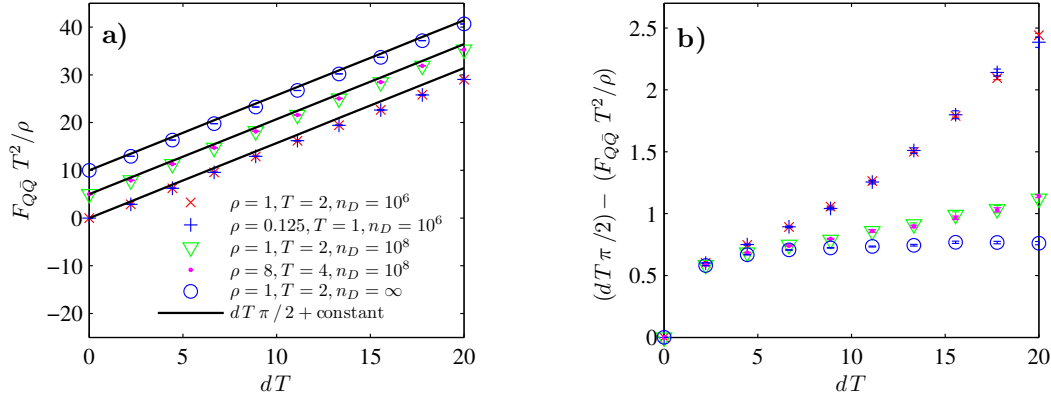


Figure 2.1: Free energy $F_{Q\bar{Q}}$ versus quark separation d in universal units for varied configuration parameters ρ , T and n_D . **a)** The essential parameters of the calculation is the dyon number n_D and the ratio ρ/T^3 . Note that the data has been shifted to irrelevant constants to make comparisons easier. **b)** The difference between the data and the analytic prediction grows for $n_D < \infty$ and reaches a constant for $n_D \rightarrow \infty$, as expected.

The final result for f_+ is

$$f_+ = I_{+,1} + I_{+,2} + V - V(S) + \Lambda. \quad (2.19)$$

2.3 Extrapolation to Infinite Volume

According to [7], f_+ does not contribute to the Polyakov loop correlator Eq. (2.1) for the infinite volume. Hence, f_- is the only contribution. Analysing the limit $V \rightarrow \infty$ (equivalently $R \rightarrow \infty$) one can use the same integrals as above. The function argument of the logarithm approaches

$$\lim_{V \rightarrow \infty} \frac{|I_{-,1} + I_{-,2} + V - V(S)|}{V} \rightarrow 1. \quad (2.20)$$

Hence, for the evaluation of the Polyakov loop correlator Eq. (2.1) the expansion $\ln(x + 1) = x + \dots$ becomes exact, yielding

$$\langle P(\mathbf{r})P(\mathbf{r}') \rangle = \frac{1}{2} \exp \left(\rho(I_{-,1} + I_{-,2} - V(S)) \right). \quad (2.21)$$

Furthermore, following the derivation in [4], the free energy may be evaluated analytically for sufficiently large d . This asymptotic result is

$$F_{Q\bar{Q}}(d) = \frac{\pi}{2} \frac{\rho}{T^2} dT, \quad (2.22)$$

which allows to approve the tendency of the numerical results.

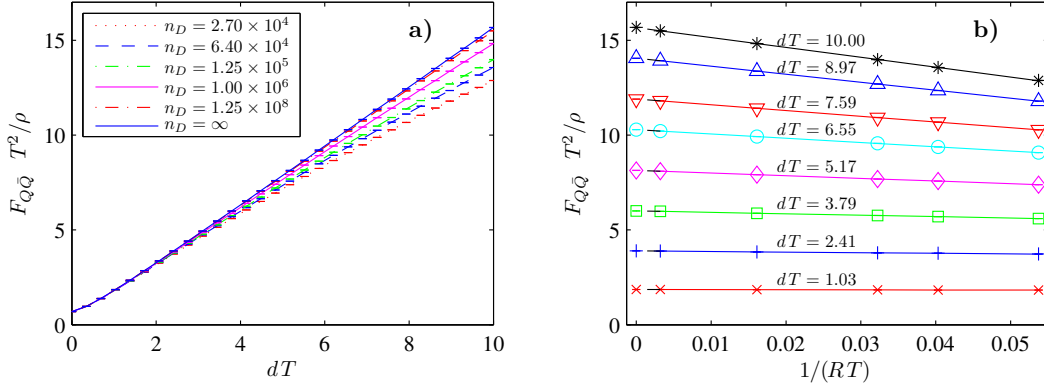


Figure 2.2: **a)** Free energy $F_{Q\bar{Q}}$ versus the quark separation d for different volumes ($T^3/\rho = 1$). **b)** Free energy $F_{Q\bar{Q}}$ versus the inverse radius of the volume. As one can see, the calculation converges to the expected value at $1/R = 0$. The radius has been calculated as $R = (3n_D/4\pi\rho)^{1/3}$.

2.4 Numerical Results

Dimensionless Units

According to [4], the slope of the free energy $F_{Q\bar{Q}}(d)$ at infinite separation and infinite volume will be

$$\sigma = \frac{\pi}{2} \frac{\rho}{T} \quad (2.23)$$

(cf. Eq. (2.22)). Therefore, I plot the free energy in units of ρ/T^2 and the quark separation in units of $1/T$. Hence, the only relevant quantities labeling different curves are the dyon number n_D and the ratio ρ/T^3 .

These statements were cross checked in Fig. 2.1a, where the free energy was calculated for three different parameter sets and is plotted against the quark antiquark separation. Note that some curves are shifted vertically to make it possible to distinguish between the different cases. As one can see, curves with the same ρ/T^3 and n_D are in agreement within their statistical errors. Furthermore, their behavior is compared to the asymptotic result of Eq. (2.22). As can be seen in Fig. 2.1b, where the difference between the asymptotic result and the numerical result is shown, this difference grows with a growing quark separation. The slope of the difference is greater for configurations of small n_D and reaches zero for $n_D = \infty$. Consequently, the numerical evaluation is in agreement with the analytical result.

Free Energy $F_{Q\bar{Q}}$

The free energy has been calculated for 6 different dyon numbers, including $n_D = \infty$. The result is shown in Fig. 2.4a, where $F_{Q\bar{Q}}$ is plotted against the quark antiquark separation. As one can see, the curves become linear at sufficiently large quark separations dT and converge to the infinite volume curve. Furthermore, the extrapolation to infinite volume is done with high accuracy in Fig. 2.4b. There, the free energy is plotted against the radius of the volume and each curve is associated to one quark separation dT . Then, linear fits

with respect to $1/(RT) \in [3 \times 10^{-3}, 5.4 \times 10^{-2}]$ were performed by means of the method of minimizing χ^2 (solid line). Afterwards an extrapolation to $1/R = 0$ was done (dashed line), showing agreement with the result of $n_D = \infty$ from Sec. 2.3.

Chapter 3

Ewald Summation

3.1 Introduction

Since an analytical solution for the Polyakov loop correlator only exists in case of non-interacting dyons, it is useful to develop a more general numerical approach. Applying it to the problem, one is able to test its efficiency and accuracy. Because the Polyakov loop correlator depends on the long range dyon potential Eq. (1.2), it is necessary that any useful method allows to evaluate this potential in an efficient way and to do a controlled extrapolation to infinite volume.

To do so, there is a rather simple approach described in [8], where n_D dyons were considered to be in a cubic spatial volume of length L . Then, observables were evaluated in a cubic spatial volume of length $\ell < L$, located at the center of the larger volume (cf. Fig. 3.1). However, this method gave rise to some negative effects. To prevent finite volume effects, one had to set $\ell \ll L$, which drastically reduces the volume, in which observables could be evaluated. Furthermore, an extrapolation to infinite volume was rather difficult, since it had to be done with respect to two parameters (ℓ and L). Another disadvantage is, that dyons tend to accumulate at the boundary of the large volume during simulations with interacting dyons.

A method for treating dyon ensembles in a way which takes care of the problems mentioned above, is Ewald's method or Ewald summation, first proposed in [9]. Ewald's method approximates infinite volume for simulations of particles with long range potentials like dyons by implementing periodic boundary conditions. One considers a cubic spatial volume of length L , filled with n_D dyons of density $\rho = n_D/L^3$. This volume is periodically repeated in every direction of space (cf. Fig. 3.2). With this setting, one can hope that finite volume effects are reduced, since the original volume is "surrounded" by dyons in all spatial directions. Furthermore, an extrapolation to infinite volume only has to be done with respect to one parameter L . Finally, the dyons will possibly not accumulate during simulations with interactions anymore. Due to these reasons, the Ewald summation seems to provide a promising ansatz to treat dyon ensembles more efficiently.

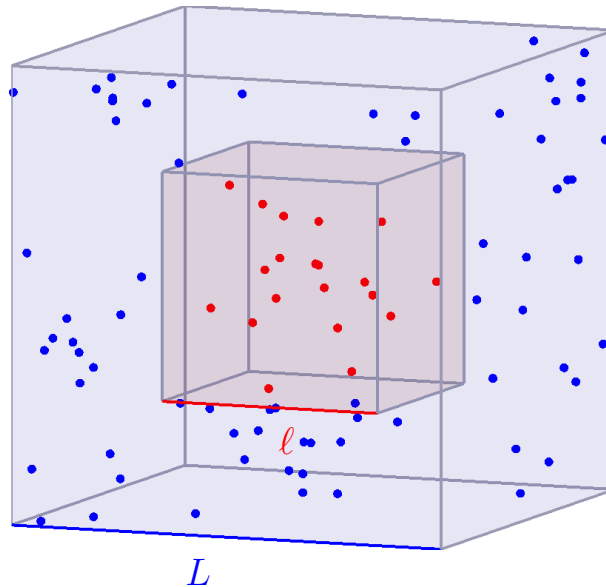


Figure 3.1: The first approach to treat dyon ensembles: locating dyons in a volume of length L (blue), but evaluating observables within a volume of length $\ell < L$ (red).

3.2 Derivation of Relevant Formulae

To compute a superposition of Coulomb-like gauge potentials at a point \mathbf{r} in the volume, one has to evaluate a sum over all dyons in the volume and all dyons in its spatial copies.

$$\Phi(\mathbf{r}) = \sum_{j=1}^{n_D} \sum_{\mathbf{n} \in \mathbb{Z}^3} \frac{q_j}{|\mathbf{r} - \mathbf{r}_j + \mathbf{n}L|} \quad (3.1)$$

This sum can not be evaluated naively, since it produces divergencies by summing infinitely often over contributions of order $1/r$ (cf. [4]). Therefore, it is split in two sums, a fast converging short range part Φ^S and a long range part Φ^L , which converges fast in Fourier space.

In the following, I will give a derivation for this splitting. Since Ewald's method can not only be used for Coulomb-like potentials, but also potentials of the form $1/r^p$, $p \in \mathbb{R}$, $p \geq 1$, I will show the general derivation. This will become relevant for studies of interacting dyons in Ch. 4, where simulations with such potentials are discussed. The derivation of Ewald's splitting for powers of the inverse dyon separation $1/r^p$ is based on the presentation in [10] and rather technical. A more physically motivated explanation for Ewald's method for $p = 1$ can be found in [11].

At first, one considers the Euler gamma function

$$\Gamma(z) = \int_0^{\infty} dt t^{z-1} \exp(-t) = r^{2z} \int_0^{\infty} dt t^{z-1} \exp(-r^2 t) \quad (3.2)$$

and the three-dimensional Gaussian distribution and its Fourier integral expansion

$$\exp(-\mathbf{r}^2 t) = \left(\frac{\pi}{t}\right)^{3/2} \int_0^{\infty} d^3 \mathbf{u} \exp(-\pi^2 \mathbf{u}^2 / t) \exp(-2\pi i \mathbf{u} \mathbf{r}), \quad (3.3)$$

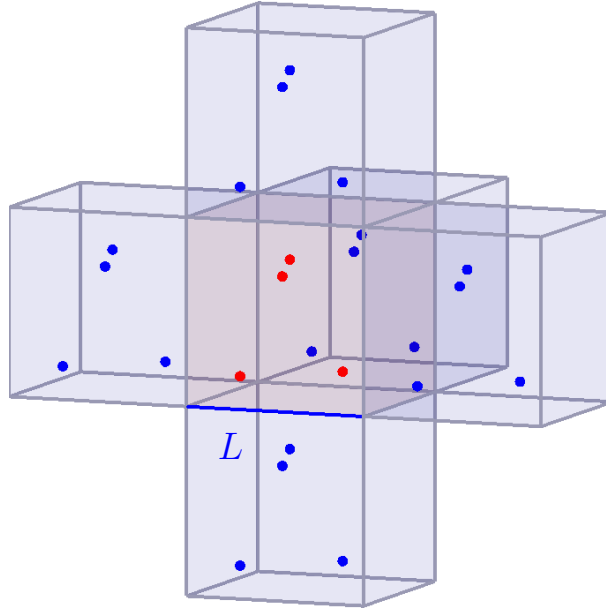


Figure 3.2: The second approach to treat dyon ensembles, used by Ewald's method and therefore studied in this chapter: locating dyons in a volume of length L and enforcing periodic boundary conditions. Observables are evaluated within the original volume (red) with respect to the infinite number of dyon copies.

where \mathbf{u} is a vector in Fourier space and \mathbf{r} is a vector in real space. Now, one sets $z = p/2$, $r = |\mathbf{r}|$ and splits the integration of the gamma function by means of an arbitrary positive parameter λ , yielding

$$\frac{\Gamma(p/2)}{r^p} = \underbrace{\int_0^{1/2\lambda^2} dt t^{p/2-1} \exp(-\mathbf{r}^2 t)}_{=I_p} + \underbrace{\int_{1/2\lambda^2}^{\infty} dt t^{p/2-1} \exp(-\mathbf{r}^2 t)}_{=J_p}. \quad (3.4)$$

This particular form of the splitting was chosen, since λ equals the standard deviation of a Gaussian for the special case of $p = 1$, where Ewald's method is associated with a Gaussian smearing of the dyons' charge distributions [11]. For the evaluation of I_p one uses the Fourier integral expansion of the Gaussian, sets $\pi^2 u^2/t = s^2$, and integrates over s first. The second integral J_p can be evaluated substituting $r^2 t = s^2$, obtaining the result

$$\frac{1}{r^p} = \frac{\pi^{3/2}}{(\sqrt{2}\lambda)^{p-3}} \int d^3\mathbf{u} f_p(\sqrt{2}\lambda\pi|\mathbf{u}|) \exp(-2\pi i\mathbf{u}\mathbf{r}) + \frac{g_p(r/\sqrt{2}\lambda)}{r^p}, \quad (3.5)$$

where

$$g_p(x) = \frac{2}{\Gamma(p/2)} \int_x^{\infty} s^{p-1} \exp(-s^2) ds \quad (3.6)$$

$$f_p(x) = \frac{2x^{p-3}}{\Gamma(p/2)} \int_x^{\infty} s^{2-p} \exp(-s^2) ds \quad (3.7)$$

lead to the exponential suppression in real and Fourier space. Now, one considers the periodic boundary conditions for a spatial volume of length L , filled with dyons fulfilling $\sum_i^{n_D} q_i = 0$. To obtain the potential at one point \mathbf{r} , it is necessary to sum over all particles and their periodical copies according to

$$\Phi_p(\mathbf{r}) = \sum_{j=1}^{n_D} \sum_{\mathbf{n} \in \mathbb{Z}^3} \frac{q_j(p)}{|\mathbf{r} - \mathbf{z}_j + \mathbf{n}L|^p}, \quad (3.8)$$

yielding the short range part

$$\Phi_p^S(\mathbf{r}) = \sum_{\mathbf{n}} \sum_j^{n_D} \frac{q_j(p)}{|\mathbf{r} - \mathbf{r}_j + \mathbf{n}L|^p} g_p \left(\frac{|\mathbf{r} - \mathbf{r}_j + \mathbf{n}L|}{\sqrt{2}\lambda} \right) \quad (3.9)$$

and the long range part

$$\Phi_p^L(\mathbf{r}) = \frac{\pi^{3/2}}{(\sqrt{2}\lambda)^{p-3}} \sum_j q_j(p) \int d^3\mathbf{u} f_p \left(\sqrt{2}\lambda\pi|\mathbf{u}| \right) \exp(-2\pi i\mathbf{u}(\mathbf{r} - \mathbf{r}_j)) \sum_{\mathbf{n}} \exp(-2\pi i\mathbf{u}\mathbf{n}L).$$

Note that the charge q may be a function of the power p , e.g. when the term of order p is obtained through the expansion of a logarithm. For the numerical computation of Φ_p^L it is necessary to evaluate the integration over the Fourier space analytically. To this end, one uses the identity

$$\sum_{\mathbf{n}} \exp(-2\pi i\mathbf{u}\mathbf{n}L) = \frac{1}{V} \sum_{\mathbf{m}} \delta \left(\mathbf{u} - \frac{\mathbf{m}}{L} \right), \quad (3.10)$$

yielding the final result

$$\Phi_p^L(\mathbf{r}) = \frac{\pi^{3/2}}{V (\sqrt{2}\lambda)^{p-3}} \sum_j \sum_{\mathbf{m}} q_j(p) f_p \left(\sqrt{2}\lambda\pi \frac{|\mathbf{m}|}{L} \right) \exp \left(-\frac{2\pi}{L} i \mathbf{m}(\mathbf{r} - \mathbf{r}_j) \right). \quad (3.11)$$

For the evaluation of the Coulombic dyon potential Eq. (3.1), the power is $p = 1$ and the charge function reads $q(p) = q$. Therefore, the relevant formulae are

$$\Phi^S(\mathbf{r}) = \sum_{\mathbf{n}} \sum_{j=1}^N \frac{q_j}{|\mathbf{r} - \mathbf{r}_j + \mathbf{n}L|} \operatorname{erfc} \left(\frac{|\mathbf{r} - \mathbf{r}_j + \mathbf{n}L|}{\sqrt{2}\lambda} \right) \quad (3.12)$$

$$\Phi^L(\mathbf{r}) = \frac{4\pi}{V} \sum_{\mathbf{k} \neq 0} \sum_{j=1}^N \frac{q_j}{k^2} e^{i\mathbf{k}(\mathbf{r} - \mathbf{r}_j)} e^{-\lambda^2 k^2 / 2}. \quad (3.13)$$

For the long range part, the sum is taken over momenta $\mathbf{k} = \frac{2\pi}{L}\mathbf{m}$, with $\mathbf{m} \in \mathbb{Z}^3$. The arbitrary parameter λ controls the trade-off between the short range and the long range part. It has to be emphasized that the sum converges only in case of a neutral configuration (such that the number of negative charges equals the number of positive charges, $\sum_j^{n_D} q_j = 0$). In this case, the divergencies of the $\mathbf{k} = 0$ term cancel. Otherwise, one had to ignore the divergencies and to neglect the $\mathbf{k} = 0$ term, which shifts the potential by a constant depending on λ (a leftover of the divergence, investigated in [12]). However, if one was interested in simulations with non-neutral charges, it would be possible to use Ewald's method, as well, since this constant does not have any physical relevance regarding to potential differences.

3.3 Detailed Description of the Algorithm

3.3.1 Computational Cost

For evaluating Polyakov loops one needs to compute the potential at $M \propto V$ points inside the volume. Obtaining these results with Ewald's method, the sum goes over all dyons and several volume copies. Therefore the scaling of this algorithm is $\mathcal{O}(V^2)$. For a better scaling, one needs the short range part to converge in the original volume. One chooses a λ , such that $\Phi^S(\mathbf{r})$ converges satisfactorily in a sphere with $r_{\max} < L/2$ and center \mathbf{r} . Furthermore, set $r_{\max} \propto \lambda$. Now let $J(\mathbf{r})$ be a set which contains all dyons or copies of dyons with $|\mathbf{r} - \mathbf{z}_j| \leq r_{\max}$. The short range part becomes

$$\Phi^S(\mathbf{r}) = \sum_{j \in J(\mathbf{r})} \frac{q_j}{|\mathbf{r} - \mathbf{z}_j|} \operatorname{erfc} \left(\frac{|\mathbf{r} - \mathbf{z}_j|}{\sqrt{2}\lambda} \right) \quad (3.14)$$

with a cost of $\mathcal{O}(V\lambda^3)$ when computed at $M \propto V$ points in the volume. The general sum for powers $p \geq 1$ is

$$\Phi_p^S(\mathbf{r}) = \sum_{j \in J(\mathbf{r})} \frac{q_j(p)}{|\mathbf{r} - \mathbf{z}_j|^p} g_p \left(\frac{|\mathbf{r} - \mathbf{z}_j|}{\sqrt{2}\lambda} \right). \quad (3.15)$$

Using the structure function $S(\mathbf{k}) = \sum_{j=1}^{n_D} q_j e^{-i\mathbf{k}\mathbf{r}_j}$ the long range part can be rewritten according to

$$\Phi^L(\mathbf{r}) = \frac{4\pi}{V} \sum_{\mathbf{k} \neq 0} e^{i\mathbf{k}\mathbf{r}} \frac{e^{-\lambda^2 \mathbf{k}^2 / 2}}{\mathbf{k}^2} S(\mathbf{k}). \quad (3.16)$$

The cost of computing the structure function is $\mathcal{O}(Vm_{\max}^3)$, where $m_{\max} \propto \frac{L}{\lambda} \propto Lk_{\max}$ is the radius of an integer sphere in Fourier space, in which the long range part has to converge. Since $S(\mathbf{k})$ does not depend on \mathbf{r} , it has to be computed only once (if the dyon positions do not change). Thus, its calculation does not contribute to the total cost. Afterwards the long range part has to be evaluated in the mentioned sphere with the cost $\mathcal{O}(Vm_{\max}^3) \propto \mathcal{O}(V(L/\lambda)^3) \propto \mathcal{O}(V^2/\lambda^3)$. The computational cost for the whole algorithm is minimized with an equal trade-off between short range and long range part. Hence we choose $\lambda \propto V^{1/6} \propto \sqrt{L}$ to obtain a total algorithm cost of $\mathcal{O}(V^{3/2})$. Note that this approach reduces the computational cost with respect to a growing volume. For an optimized computation for a constant volume, it is necessary to vary λ and to compare the trade-off between short range and long range part, which was done in [4].

3.3.2 Technical Aspects

Short Range Part

For an effective algorithm it is necessary to reach dyons in the sphere without iterating over all dyons in the volume. Therefore, one divides the original volume in cubic subvolumes. These subvolumes contain dyons. Technically, the volume is a list of subvolumes now, containing lists of pointers to the dyons located in these subvolumes. For a point \mathbf{r} in the volume one can calculate the position of the subvolume and address all subvolumes

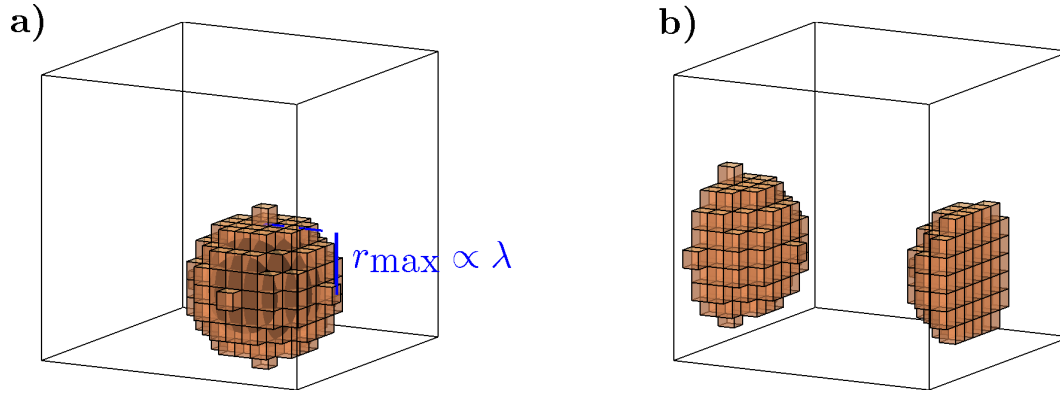


Figure 3.3: LEGO™ sphere in different situations. Here, one cube is considered to be a subvolume of length a . **a)** The LEGO™ sphere is larger than the requested sphere with radius r_{\max} to reach all dyons. **b)** Integer values of the LEGO™ sphere are shifted periodically.

in a sphere with radius r_{\max} to reach the relevant dyon positions. Hence, procedures were implemented to get integer vectors for an approximated sphere of subvolume copies, called “LEGO™ sphere” in the following, as can be seen in Fig. 3.3a. The size of one subvolume has to be defined by a lattice parameter a . Note that the LEGO™ sphere’s radius is larger than the actual radius r_{\max} to ensure the consideration of all dyons in the sphere. Since points \mathbf{r} near the boundary reach into neighbour volumes, one needs to shift the LEGO™ sphere periodically and shift the positions of their containing dyons, as well (Fig. 3.3b).

Long Range Part

Since the summation over momenta \mathbf{k} is symmetric with respect to $\mathbf{k} = 0$, it is unnecessary to sum over a whole sphere of reciprocal volume copies. The momenta are proportional to integer vectors $\mathbf{m} = (i, l, j)$. Then, the condition for a symmetric half sphere of integer values with radius m_{\max} is

$$\left\{ i > 0 \vee \left[(i = 0) \wedge (l > 0) \wedge (j \geq 0) \right] \vee \left[(i = 0) \wedge (l \leq 0) \wedge (j > 0) \right] \right\} \wedge |\mathbf{m}| \leq m_{\max}. \quad (3.17)$$

An illustration of this condition can be seen in Fig. 3.4. Momenta fulfilling it shall be named \mathbf{k}_{Sym} . Now, the long range part reduces to

$$\Phi^L(\mathbf{r}) = \frac{4\pi}{V} \sum_{\mathbf{k}_{\text{Sym}}} \frac{2e^{-\lambda^2 \mathbf{k}^2 / 2}}{\mathbf{k}^2} \text{Re} \left(e^{i\mathbf{k}\mathbf{r}} S(\mathbf{k}) \right). \quad (3.18)$$

The general long range part for powers $p \geq 1$ reads

$$\Phi^L(\mathbf{r}) = \frac{\pi^{3/2}}{V (\sqrt{2}\lambda)^{p-3}} \sum_{j=1}^{n_D} \sum_{\mathbf{k}_{\text{Sym}}} 2f_p \left(\frac{\lambda k}{\sqrt{2}} \right) \text{Re} \left(e^{i\mathbf{k}\mathbf{r}} S(\mathbf{k}, p) \right). \quad (3.19)$$

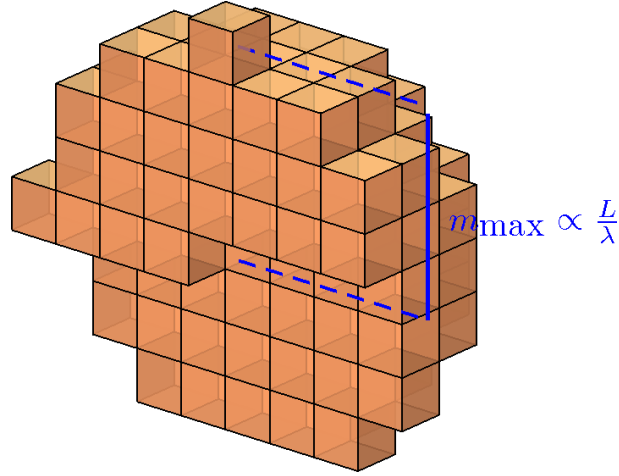


Figure 3.4: Volume copies for symmetric sum of long range part (here, one cube is considered to be a copy of the original volume). Note that $\mathbf{m} = 0$ in the center of the sphere is already neglected.

3.4 Numerical Results for Dyon Ensembles

The implemented algorithms were tested in [13], yielding agreement with the predicted scaling of $\mathcal{O}(V^{3/2})$. Furthermore, they were used to evaluate the Polyakov loop correlator for numerous configurations in [4]. The results regarding the free energy in case of non-interacting dyons can be seen in Fig. 3.4a, where computations have been done for four different volumes ($LT \in \{20, 30, 40, 50\}$, equivalently to $\frac{n_D}{10^3} \in \{8, 27, 64, 125\}$). There, the free energy is plotted against the quark separation with $\rho/T^3 = 1$. As one can see, the curves grow linearly at sufficiently large quark separations dT and seem to converge to an infinite volume curve with growing LT . Since we are interested in the use of Ewald's method as a tool for extrapolating to infinite volume, it is necessary to study this convergence behavior. In Fig. 3.4b, one can see the free energy $F_{Q\bar{Q}}$ versus the inverse length of the volume for $dT \in [0.2, 2.0]$. Since the data points in Fig. 3.4a are not all at the same dT , the points in Fig. 3.4b are obtained via interpolation. Afterwards, the extrapolation is done via resampling of the existing data for $LT \in \{20, 30, 40, 50\}$ with $N = 500$ and performing linear fits with the method of minimizing χ^2 . After fitting, the mean at $1/L = 0$ was calculated, as well as the standard deviation $\sigma_{L^{-1}=0} = \sqrt{\text{Var}[F_{Q\bar{Q}}(L^{-1} = 0)]}$, which is taken as statistical error. The colored point for $1/L = 0$ is the analytical prediction at infinite volume (cf. Ch. 2).

The extrapolation and the analytical prediction are compared in Fig. 3.4c,d, as well. As one can see, the extrapolated values are clearly in agreement considering a confidence interval of 95% (a statistical error of 2σ).

The final conclusion is, that Ewald's method is an elegant and efficient method to treat objects of long range potential such as dyons. It seems to be the method of choice for further treatments of interacting dyons.

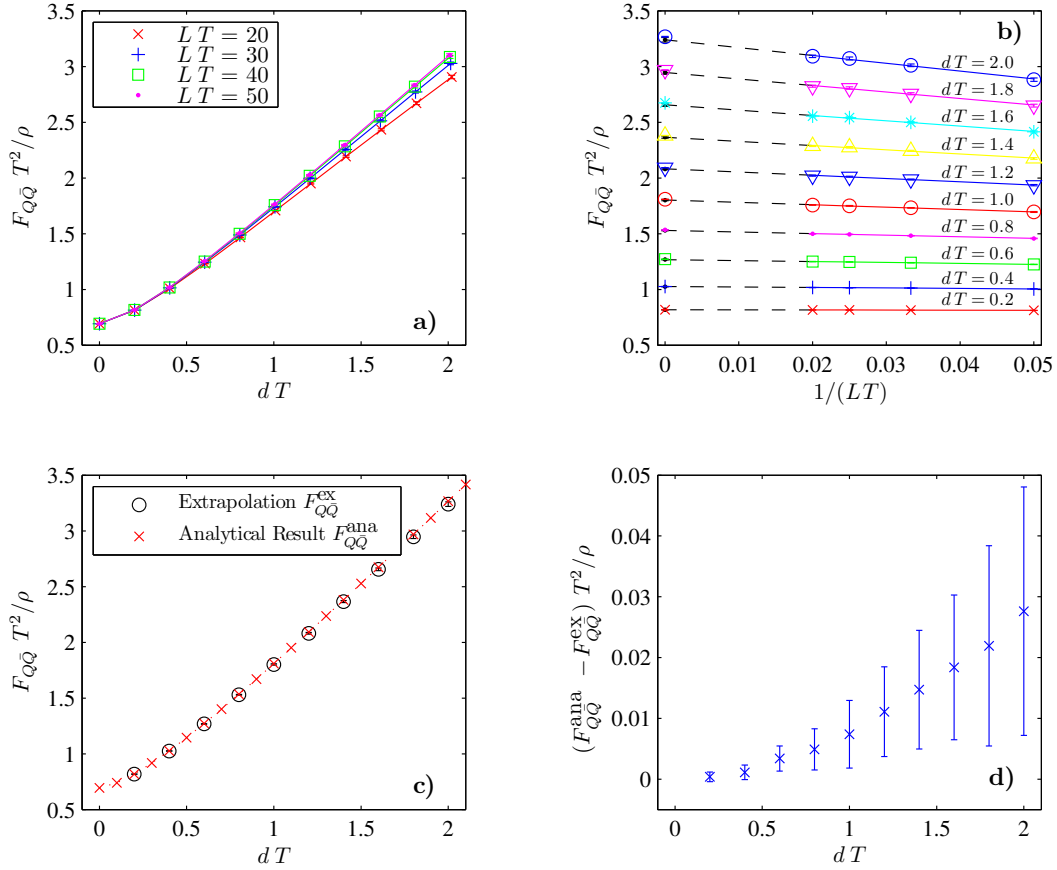


Figure 3.5: **a)** Free energy $F_{Q\bar{Q}}$ versus quark separation for four lengths of the main volume. All data was obtained using $T^3/\rho = 1$. **b)** Free energy $F_{Q\bar{Q}}$ versus the inverse length of the volume for different separations dT and extrapolation to $(LT)^{-1} = 0$. The solid curves are the fit functions in the fit regions, whereas the dashed line marks the extrapolations. **c)** Comparison between analytical result and extrapolation. **d)** Difference between analytical result and extrapolation.

Chapter 4

Computing the Effective Action of Interacting Dyons

To describe interactions of dyons and to evaluate observables using the path integral approach, it is necessary to define an integration measure and therefore a metric for n_D interacting dyons. As described in [8], the approximate moduli space metric G proposed in [3] is only valid for a small number of dyon configurations, since its positive definiteness is violated in most cases. In the following, I summarize an approach to approximate a moduli space metric by means of two-body interactions, first proposed in [5, 6], where the positive definiteness is ensured. This is essential for Monte Carlo simulations, as well.

4.1 Effective Action

As described in [8], the integration measure for interacting multi-dyon configurations of positions $\{\mathbf{r}_k\}$ is given by

$$\left(\prod_{k=1}^{n_D} d^3 r_k \right) \det(G), \quad (4.1)$$

with G being the moduli space metric. This metric is known exactly for two dyons with indices i, j of different charge, which is essentially a caloron [2]. Furthermore, for two dyons of the same charge, one can use the approximate moduli space metric proposed in [3]. Combining both results yields an approximate moduli space metric

$$G_{(i,j)} = \begin{pmatrix} 2\pi - \frac{2q_i q_j}{T|\mathbf{r}_i - \mathbf{r}_j|} & \frac{2q_i q_j}{T|\mathbf{r}_i - \mathbf{r}_j|} \\ \frac{2q_i q_j}{T|\mathbf{r}_i - \mathbf{r}_j|} & 2\pi - \frac{2q_i q_j}{T|\mathbf{r}_i - \mathbf{r}_j|} \end{pmatrix}, \quad (4.2)$$

with eigenvalues

$$\lambda_1 = 2\pi \quad (4.3)$$

$$\lambda_2 = 2\pi - \frac{4q_i q_j}{T|\mathbf{r}_i - \mathbf{r}_j|}. \quad (4.4)$$

Since the metric is positive definite only for dyons of different charge or dyons of the same charge at separations $> \frac{2}{\pi T}$, I demand the configurations to be of “hard core”, where

dyons of same charge may not come closer than $\frac{2}{\pi T}$. Now, the determinant of the moduli space metric of a dyon configuration with n_D dyons is approximated by the product of the determinants of Eq. (4.2) for all pairs (i, j) of the configuration, yielding

$$\begin{aligned} \prod_{(i,j)} \det(G_{(i,j)}) &= \prod_{(i,j)} 4\pi^2 \left(1 - \frac{2q_i q_j}{\pi T |\mathbf{r}_i - \mathbf{r}_j|} \right) \\ &= (4\pi^2)^{n_D^2} \exp \left[\sum_{(i,j)} \ln \left(1 - \frac{2q_i q_j}{\pi T |\mathbf{r}_i - \mathbf{r}_j|} \right) \right]. \end{aligned} \quad (4.5)$$

With this procedure, the multi-dyon interaction is approximated by a sum over two-body forces. One is now able to evaluate the expectation values of observables O using path integrals

$$\langle O \rangle = \frac{1}{Z} \int \left(\prod_{k=1}^{n_D} d^3 r_k \right) O(\{\mathbf{r}_k\}) \exp [S(\{\mathbf{r}_k\})] \quad (4.6)$$

$$Z = \int \left(\prod_{k=1}^{n_D} d^3 r_k \right) \exp [S(\{\mathbf{r}_k\})] \quad (4.7)$$

with the effective action

$$S(\{\mathbf{r}_k\}) = \frac{1}{2} \sum_{i=1}^{n_D} \sum_{j=1, j \neq i}^{n_D} \ln \left(1 - \frac{2q_i q_j}{\pi T |\mathbf{r}_i - \mathbf{r}_j|} \right), \quad (4.8)$$

where the sum goes twice over all dyon pairs and therefore is multiplied with the factor $1/2$.

4.2 Periodicity

Since the action Eq. (4.8) is proportional to $1/r$ in the limit of large dyon separations, one expects the same problems to arise as for calculating the dyon potential (finite volume effects, boundary effects, cf. Ch. 3). Therefore I apply Ewald's method to the effective action. As mentioned in section Sec. 3.2, one is able to use Ewald's method even for higher powers of inverse separation. Therefore one performs an expansion of Eq. (4.8) in powers of $1/r_{ij}$, where $r_{ij} = |\mathbf{r}_i - \mathbf{r}_j|$, yielding

$$S^N = \frac{1}{2} \sum_{i \neq j} \left(-\frac{2q_i q_j}{\pi T r_{ij}} - \frac{2(q_i q_j)^2}{(\pi T r_{ij})^2} - \frac{8(q_i q_j)^3}{3(\pi T r_{ij})^3} + \mathcal{O} \left(\frac{1}{r_{ij}^4} \right) \right). \quad (4.9)$$

The superscript “ N ” denotes the non-periodic kind of the sum. Now, it is possible to calculate the action to any order $p \in \mathbb{N}$ by means of Ewald's method. Every term of the expansion of order $1/r^l$ can be derived following the approach for interaction energies in [11]. It has to be emphasized, that the Ewald summation of the interaction quantity $S_{(l)}$

is done slightly different compared to calculations of the potential, namely

$$S_{(l)}^S = c_{(l)} \frac{1}{2} \sum_{i=1}^{n_D} q_i^l \Phi_{(l), \text{dyon separation} \neq 0}^S(\mathbf{r}_i) \quad (4.10)$$

$$= c_{(l)} \frac{1}{2} \sum_{j \in J(\mathbf{r}_i)} \sum_{i=1}^{n_D} \frac{q_i^l q_j^l}{|\mathbf{r}_i - \mathbf{z}_j|^l} g_l \left(\frac{|\mathbf{r}_i - \mathbf{z}_j|}{\sqrt{2}\lambda} \right) \quad (4.11)$$

$$S_{(l)}^L = c_{(l)} \frac{1}{2} \sum_{i=1}^{n_D} q_i^l \Phi_{(l)}^L(\mathbf{r}_i) \quad (4.12)$$

$$= c_{(l)} \frac{\pi^{3/2}}{2V (\sqrt{2}\lambda)^{l-3}} \sum_{j=1}^{n_D} \sum_{\mathbf{k}_{\text{Sym}}} f_l \left(\frac{\lambda k}{\sqrt{2}} \right) (2|S(\mathbf{k}, l)|^2), \quad (4.13)$$

referring to the quantities in Sec. 3.2 and with the corresponding factor $c_{(l)}$ of the expansion in Eq. (4.9). Furthermore the summation over dyon separations $r_{ii} = 0$ in the long range part leads to a self interaction term. However, this term only depends on the trade-off parameter λ and the dyon number n_D and therefore is merely a constant which is irrelevant during a Monte Carlo simulation. A second constant is produced by the neglect of the $\mathbf{k} = 0$ term for even orders l , as described in Sec. 3.1, but this constant is irrelevant, as well. Thus, a periodic action of order p can be defined as

$$S_p^P = \sum_{l=1}^p (S_{(l)}^S + S_{(l)}^L). \quad (4.14)$$

In addition to this, a second structure function is needed for even powers of l , which are independent of charges. It is defined as $S'(\mathbf{k}) = \sum_{i=1}^{n_D} e^{-i\mathbf{k}\mathbf{r}_i}$. The short and long range parts for the periodic action are then

$$S_{(1)}^S = -\frac{1}{\pi} \sum_{i=1}^{n_D} \sum_{j \in J(\mathbf{r}_i)} \frac{q_i q_j}{T |\mathbf{r}_i - \mathbf{z}_j|} \operatorname{erfc} \left(\frac{|\mathbf{r}_i - \mathbf{z}_j|}{\sqrt{2}\lambda} \right), \quad (4.15)$$

$$S_{(1)}^L = -\frac{8}{TV} \sum_{\mathbf{k}_{\text{Sym}}} |S(\mathbf{k})|^2 \frac{\exp\left(-\frac{\lambda^2 \mathbf{k}^2}{2}\right)}{\mathbf{k}^2}, \quad (4.16)$$

$$S_{(2)}^S = -\frac{1}{\pi^2} \sum_{i=1}^{n_D} \sum_{j \in J(\mathbf{r}_i)} \frac{\exp\left(-\frac{|\mathbf{r}_i - \mathbf{z}_j|^2}{2\lambda^2}\right)}{T^2 |\mathbf{r}_i - \mathbf{z}_j|^2}, \quad (4.17)$$

$$S_{(2)}^L = -\frac{4}{T^2 V} \sum_{\mathbf{k}_{\text{Sym}}} |S'(\mathbf{k})|^2 \frac{\operatorname{erfc}\left(\frac{\lambda k}{\sqrt{2}}\right)}{k}, \quad (4.18)$$

$$S_{(3)}^S = -\frac{4}{3\pi^3} \sum_{i=1}^{n_D} \sum_{j \in J(\mathbf{r}_i)} q_i q_j \left(\frac{\operatorname{erfc}\left(\frac{|\mathbf{r}_i - \mathbf{z}_j|}{\sqrt{2}\lambda}\right)}{T^3 |\mathbf{r}_i - \mathbf{z}_j|^3} + \sqrt{\frac{2}{\pi}} \frac{\exp\left(-\frac{|\mathbf{r}_i - \mathbf{z}_j|^2}{2\lambda^2}\right)}{T^3 \lambda |\mathbf{r}_i - \mathbf{z}_j|^2} \right), \quad (4.19)$$

$$S_{(3)}^L = -\frac{16}{3\pi^2 T^3 V} \sum_{\mathbf{k}_{\text{Sym}}} |S(\mathbf{k})|^2 \left(-\operatorname{Ei} \left(-\frac{k^2 \lambda^2}{2} \right) \right), \quad (4.20)$$

with the exponential integral $\operatorname{Ei}(x) = -\int_{-x}^{\infty} \frac{e^{-t}}{t} dt$. Other quantities are explained in Ch. 3.

4.3 Logarithmic Behavior for Small Separations

Due to the $1/r$ -expansion, which is valid for large separations, the logarithmic core of Eq. (4.8) is not represented in a satisfying way by Eq. (4.14) for small separations. One of the most important properties of this core is, that dyons of same charge may not come closer than $r = 2/\pi T$, as explained at the beginning of this chapter. Therefore I correct the periodic Ewald result within a sphere of radius r_C by replacing it with the logarithmic core, as described in the following. This seems to be a valid procedure, as investigations showed in [12].

The result of Ewald's method S^P is approximately equal to the result S^N of the non-periodic expansion in $1/r$ in Eq. (4.9) for rather small separations. Furthermore S^N becomes equal to the non-periodic logarithmic S for rather large separations. To get a sufficiently smooth connection at the boundary of the sphere, I subtract S^N from the periodic result and add S of Eq. (4.8), yielding the correction term

$$S_p^{\text{Corr}} = \frac{1}{2} \sum_{j=1}^{n_D} \sum_{i \in I(\mathbf{r}_j)} \left[\sum_{l=1}^p S_{(l)}^N(q_i q_j, |\mathbf{r}_j - \mathbf{z}_i|) - \ln \left(1 - \frac{2q_i q_j}{\pi T |\mathbf{z}_i - \mathbf{r}_j|} \right) \right], \quad (4.21)$$

where the notation $S_{(l)}^N$ stands for the l^{th} -order term in the series expansion of the logarithm. The action is

$$S = S_p^P - S_p^{\text{Corr}}. \quad (4.22)$$

To reach an algorithm of the same order as the short range sum, the summation is done over all dyons j in the volume and over dyons in a set $I(\mathbf{r}_j)$, which contains all dyons or copies of dyons within a sphere $|\mathbf{r}_j - \mathbf{z}_i| < r_C$, addressed by the LEGOTM sphere-algorithm. For an efficient computing, the cut-off radius r_C should not be greater than the radius of the short range-sphere r_{max} .

Now, it is possible to estimate the behavior of S_p^{Corr} depending on the cut-off radius r_C . This is useful to analyze the optimal expansion order p for an optimal trade-off between efficiency and precision. Starting with Eq. (4.21) and with an expansion of the logarithm yields

$$S_1^{\text{Corr}} = \frac{1}{2} \sum_j^{n_D} \sum_{i \in I(\mathbf{r}_j)} \left[-\frac{2q(\mathbf{z}_i)q(\mathbf{r}_j)}{\pi T |\mathbf{z}_i - \mathbf{r}_j|} - \left(-\frac{2q(\mathbf{z}_i)q(\mathbf{r}_j)}{\pi T |\mathbf{z}_i - \mathbf{r}_j|} - \frac{2}{\pi^2 T^2 |\mathbf{z}_i - \mathbf{r}_j|^2} + \mathcal{O} \left(\frac{1}{|\mathbf{z}_i - \mathbf{r}_j|^3} \right) \right) \right] \quad (4.23)$$

$$= \frac{1}{2} \sum_j^{n_D} \sum_{i \in I(\mathbf{r}_j)} \frac{2}{\pi^2 T^2 |\mathbf{z}_i - \mathbf{r}_j|^2} + \mathcal{O} \left(\frac{1}{|\mathbf{z}_i - \mathbf{r}_j|^3} \right). \quad (4.24)$$

This sum can be estimated by an integral over the dimensionless volume

$$S_{1,\text{ana}}^{\text{Corr}} = \frac{1}{2} \int d^3(T\mathbf{r}_j) \int_{|\mathbf{r}_j - \mathbf{z}_i| < r_C} d^3(T\mathbf{z}_i) \frac{2}{\pi^2 T^2 |\mathbf{z}_i - \mathbf{r}_j|^2}. \quad (4.25)$$

Now one performs a coordinate transformation to relative coordinates $\mathbf{R} = \frac{1}{2}(\mathbf{z}_i + \mathbf{r}_j)$,

$\mathbf{r} = \mathbf{z}_i - \mathbf{r}_j$. The Jacobian of this transformation is 1.

$$S_{1,\text{ana}}^{\text{Corr}} = \frac{1}{\pi^2} \int_{T^3V} d^3(T\mathbf{R}) \int_{r < r_C} d^3(T\mathbf{r}) \frac{1}{(Tr)^2} \quad (4.26)$$

Since the first integral is a constant over the volume, the result is a factor T^3V . The second integral is over a sphere with radius Tr_C , arriving at

$$S_{1,\text{ana}}^{\text{Corr}} = \frac{1}{\pi^2} T^3V \int_0^{Tr_C} 4\pi(Tr)^2 d(Tr) \frac{1}{(Tr)^2} \quad (4.27)$$

$$= \frac{4}{\pi} T^4 V r_C. \quad (4.28)$$

This estimation is possible for higher orders, as well. At order $p = 2$, the sum depends on the charge product of two dyons $q(\mathbf{r}_i)q(\mathbf{r}_j)$

$$S_2^{\text{Corr}} = \frac{1}{2} \sum_j^{n_D} \sum_{i \in I(\mathbf{r}_j)} \frac{8q(\mathbf{r}_1)q(\mathbf{r}_2)}{3\pi^3 T^3 |\mathbf{r}_i - \mathbf{r}_j|^3} + \mathcal{O}\left(\frac{1}{r^4}\right) \quad (4.29)$$

$$S_{2,\text{ana}}^{\text{Corr}} = \frac{16}{3\pi^2} \int_{T^3V} d^3(T\mathbf{R}) \int_{r < r_C} d(Tr) \frac{q(\mathbf{r}_i)q(\mathbf{r}_j)}{Tr}. \quad (4.30)$$

Therefore there seems to be no simple way to evaluate the estimation integral analytically. But since the volume is of neutral charge, i.e. $\sum_i^{n_D} q_i = 0$, one can hope that for rather large r_C , S_2^{Corr} becomes negligible in comparison to higher odd orders due to cancellations.

Again, for order $p = 3$, the estimation of S^{Corr} can be done, yielding

$$S_{3,\text{ana}}^{\text{Corr}} = -\frac{8T^2}{\pi^3} V \frac{1}{r_C} + \text{const.} \quad (4.31)$$

The constant seems to be configuration specific and represents the correction term for $r_C \rightarrow \infty$. Therefore, one can assume, that an optimal precision of the correction method would be achieved for $r_C \rightarrow \infty$.

To test these estimations, procedures for the evaluation of the quantity S_p^{Corr} (Eq. (4.21)) were implemented. Using these, the correction terms have been computed numerically with respect to growing r_C for various configurations and are shown in Fig. 4.1 in comparison to the analytical estimations. Note that the curves of S_2^{Corr} and S_3^{Corr} have been shifted to $-S_p^{\text{Corr}}(r_C^{\text{max}}) - \frac{8T^2V}{\pi^3 r_C^{\text{max}}}$, to get rid of the configuration specific constant. Doing so, a statistical evaluation is possible. As one can see, the correction term of order $p = 1$ diverges with growing r_C . Thus, it seems doubtful whether such a correction will be sufficient to generate meaningful results. At order $p = 2$ and $p = 3$ the correction terms reach a plateau with growing r_C . As expected, the correction term of the even order $p = 2$ is negligible in comparison to the next highest order. However, the results at $p = 2$ fluctuate more than these at $p = 3$ due to contributions depending on the charge product. Hence, the optimal precision would be achieved for $p = 3$ at $r_C \rightarrow \infty$, yielding a configuration specific constant S^α . For order $p = 3$ this constant is given by

$$S_3^\alpha = S_3^{\text{Corr}} + \frac{8T^2}{\pi^3} V \frac{1}{r_C} + \mathcal{O}\left(\frac{1}{r_C^2}\right). \quad (4.32)$$

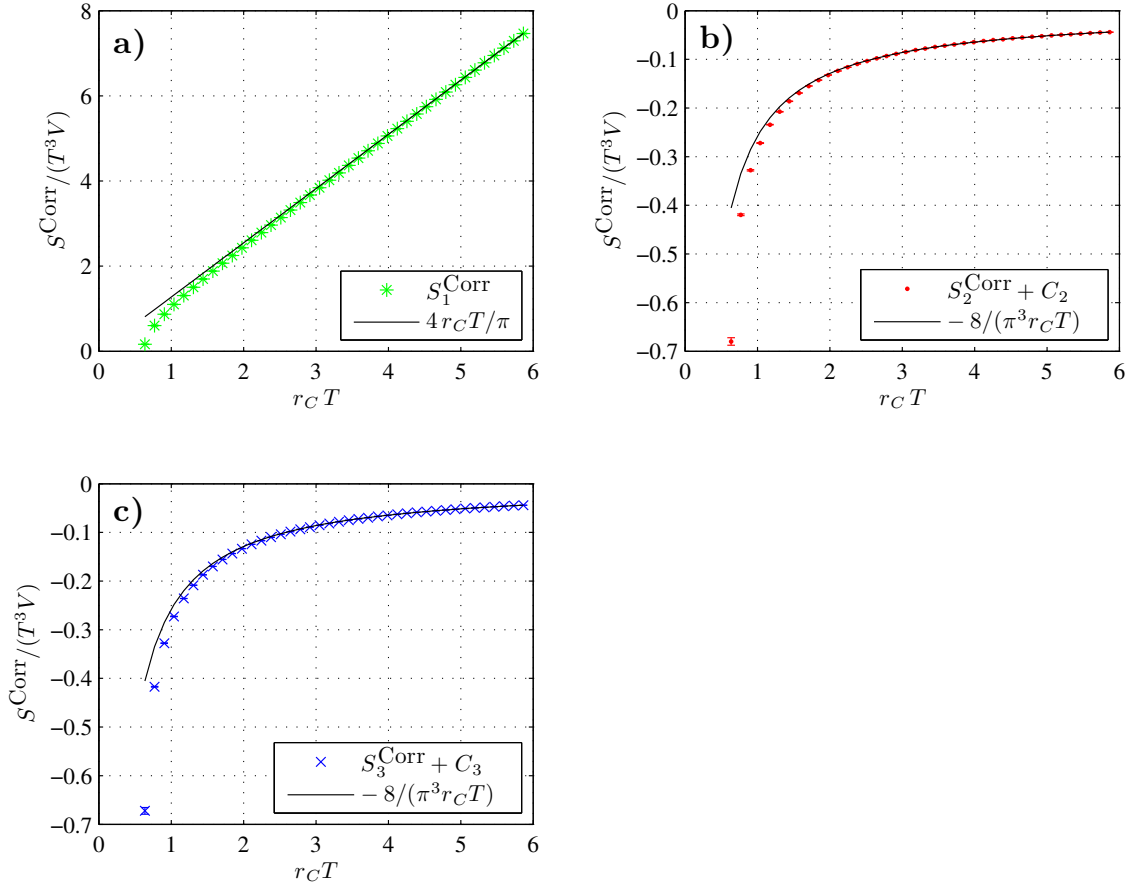


Figure 4.1: Correction terms S_p^{Corr} with respect to the cut-off radius r_C . The data shown in this figure was obtained using 30 configurations of $n_D = 400$ with $\rho/T^3 = 1$. The correction terms are compared to the analytical curves. Note that each S_2^{Corr} and S_3^{Corr} were shifted by a constant $C_p = -S_p^{\text{Corr}}(r_C^{\text{max}}) - \frac{8VT^2}{\pi^3 r_C^{\text{max}}}$, to get rid of the configuration specific constant. Hence, the possibility of a statistical treatment is ensured.

Summing up the results of this section, the final formula for the computation of the effective action with logarithmic core is

$$S^{\text{Log}} = S_3^P - S_3^\alpha \quad (4.33)$$

$$= \sum_{l=1}^3 \left(S_{(l)}^S + S_{(l)}^L \right) - S_3^{\text{Corr}} - \frac{8T^2}{\pi^3} V \frac{1}{r_C}. \quad (4.34)$$

The error of this procedure is expected to be of order $\mathcal{O}(1/r_C^2)$, respectively $\mathcal{O}(1/r_C^3)$, if one takes cancellations at order $1/r_C^2$ into account (cf. the cancellations in Eq. (4.29)).

4.4 Metropolis Algorithm

Since an efficient algorithm for computing the action is known now, one can continue adjusting the algorithm for the computation of the difference of the action ΔS^{Log} with respect to a Monte Carlo step in a Metropolis algorithm. This is necessary to produce

configurations following the distribution $\exp(S^{\text{Log}})$, and therefore to efficiently obtain expectation values of observables using Eq. (4.6).

Doing one Monte Carlo step, the position of dyon j is shifted by a random three-dimensional vector to $\mathbf{r}'_j = \mathbf{r}_j + \mathbf{\Delta}$. The difference for every quantity β is defined as

$$\Delta S^\beta = S^\beta(\mathbf{r}_j + \mathbf{\Delta}) - S^\beta(\mathbf{r}_j). \quad (4.35)$$

For the long range part, one has to update the structure functions according to

$$S(\mathbf{k}, \mathbf{r}_j + \mathbf{\Delta}) = S(\mathbf{k}) + q_j \left(e^{-i\mathbf{k}(\mathbf{r}_j + \mathbf{\Delta})} - e^{-i\mathbf{k}\mathbf{r}_j} \right), \quad (4.36)$$

$$S'(\mathbf{k}, \mathbf{r}_j + \mathbf{\Delta}) = S'(\mathbf{k}) + \left(e^{-i\mathbf{k}(\mathbf{r}_j + \mathbf{\Delta})} - e^{-i\mathbf{k}\mathbf{r}_j} \right) \quad (4.37)$$

and to evaluate $S_{(l)}^L$ again. This means a computational cost of $\mathcal{O}(V/\lambda^3)$. Furthermore, regarding the update of a whole configuration, the cost is $\mathcal{O}(V^2/\lambda^3)$.

The short range part difference can be evaluated to

$$\Delta S_3^S = \sum_{l=1}^3 \left[\sum_{i \in I(\mathbf{r}_j + \mathbf{\Delta})} S_{(l)}^S(|\mathbf{r}_j + \mathbf{\Delta} - \mathbf{z}_i|) - \sum_{i \in I(\mathbf{r}_j)} S_{(l)}^S(|\mathbf{r}_j - \mathbf{z}_i|) \right], \quad (4.38)$$

which means a computational cost of $\mathcal{O}(\lambda^3)$. Updating the whole configuration is associated with a cost of $\mathcal{O}(V\lambda^3)$.

Finally, the correction term difference ΔS^{Corr} may be evaluated in the same kind as the short range part difference (with less or equal cost, if $r_C \leq r_{\text{max}}$). Furthermore, S^{Corr} is the only relevant correction quantity, since $\Delta S_3^\alpha = \Delta S_3^{\text{Corr}}$.

Summing up the differences, the formula for calculating the action difference is

$$\Delta S^{\text{Log}} = \sum_{l=1}^3 \left(S_{(l)}^L(\mathbf{r}_j + \mathbf{\Delta}) - S_{(l)}^L(\mathbf{r}_j) \right) + \Delta S_3^S - \Delta S_3^{\text{Corr}}. \quad (4.39)$$

Again, choosing $\lambda \propto \sqrt{L}$, the computational cost for updating the whole configuration is $\mathcal{O}(V^{3/2})$.

Chapter 5

Summary and Outlook

In this work I studied several aspects of simulating and computing observables in dyon models.

At first, analytical expressions for obtaining the Polyakov loop correlator in case of non-interacting dyons were evaluated numerically. Using the results I was able to obtain the free energy $F_{Q\bar{Q}}$ between a static quark antiquark pair, which is linear for growing quark separations. The results showed, that even the non-interacting model of dyons generates confinement.

Secondly, the Ewald summation was studied, a numerical method to treat dyon ensembles with finite volume effects under better control, reached through periodic boundary conditions. The free energy obtained by means of this method was linear for growing quark separations, as well. An extrapolation to infinite volume showed agreement with the results obtained through the analytical approach. Hence, I was able to show, that the Ewald summation is an efficient numerical method to treat dyon ensembles.

The third aspect approximates interactions in multi-dyon configurations using two body interactions, resulting in an “effective action”, applicable for Monte Carlo simulations. This action was evaluated by means of Ewald’s method to keep problems such as finite volume and boundary effects under control. Furthermore, a Metropolis algorithm with respect to this action was outlined.

The obtained insights will be of essential importance when studying models of interacting dyons more precisely. To do so, the algorithm for calculating the effective action of the approximate interaction model has to be implemented. With the results obtained through this algorithm, one should be able to obtain more insights regarding interacting dyons and the dyon model in general, which perhaps will contribute to our understanding of confinement.

Bibliography

- [1] J. Schwinger, “A Magnetic Model of Matter”, *Science* 165 (3895): 757 (1969)
- [2] T. C. Kraan, ”‘Instantons, monopoles and toric hyper-Kaehler manifolds’”, *Commun. Math. Phys.* **212**, 503 (2000) [arXiv:hep-th/9811179]
- [3] D. Diakonov and V. Petrov, *Phys. Rev.* **D76**, 056001 (2007), 0704.3181.
- [4] F. Bruckmann, S. Dinter, E.-M. Ilgenfritz, B. Maier, M. Müller-Preussker, and M. Wagner, unpublished notes (2011)
- [5] F. Bruckmann, S. Dinter, E.-M. Ilgenfritz, M. Müller-Preussker, and M. Wagner, private communication (2009)
- [6] S. Dinter, diploma thesis, “Simulation of Dyon Models in SU(2) Yang-Mills Theory” (2009)
- [7] M. Wagner, private notes (2011)
- [8] F. Bruckmann, S. Dinter, E.-M. Ilgenfritz, M. Müller-Preussker, and M. Wagner, *Phys. Rev.* **D79**, 116007 (2009), 0903.3075.
- [9] P. Ewald, “Die Berechnung optischer und elektrostatischer Gitterpotentiale”, *Ann. Phys.* **369**, 253-287 (1921).
- [10] U. Essmann, L. Perera, M. L. Berkowitz, T. Darden, H. Lee, L. G. Pedersen, “A smooth particle mesh Ewald method,” (1995).
- [11] H. Lee, W. Cai, “Ewald summation for Coulomb interactions in a periodic supercell,” (2009).
- [12] B. Maier, Internship Report ”‘Effiziente Berechnung von periodischen Potentialen und Feldern inverser r -Potenzen durch Ewaldsummation’” (2010)
- [13] B. Maier, Internship Report ”‘Berechnen der A_0 -Komponente von Dyonfeldern mithilfe von Ewald-Summation’” (2010)
- [14] F. Bruckmann, private notes (2011)

Danksagung

Während der Entstehung dieser Arbeit wurde ich von einer Reihe von Personen unterstützt, ohne die selbige nicht erfolgreich hätte bearbeitet werden können.

Zuerst möchte ich Dr. Marc Wagner danken, der den Entstehungsprozess meiner Arbeit nunmehr anderthalb Jahre kompetent betreute, unzählige Denkanstöße gab, physikalisch stets anschaulich und verständlich erklärte und ein angenehmer und unterhaltsamer Büronachbar war. Ich freue mich deshalb sehr auf weitere Kollaborationen in den kommenden Jahren.

Prof. Michael Müller-Preußker danke ich für die Möglichkeit, mich in seiner Arbeitsgruppe schon früh und konstant aktiv an Forschung beteiligen zu können, sowie für seine kompetente Beratung, die nicht nur fachlich half, sondern auch für die Zusammenarbeit in Gremien der Universitätsstrukturen oft von essentieller Bedeutung war. Nicht zuletzt danke ich ihm für den Vorschlag als Stipendiat der Studienstiftung des deutschen Volkes, aufgrund dessen ich Zugang zu einem ausgezeichneten Netzwerk engagierter Menschen erhielt und Sorgen materieller Natur vorerst der Vergangenheit angehören. Im gleichen Atemzug möchte ich daher auch der Studienstiftung für die Unterstützung danken.

Weiterhin gebührt Simon Dinter Dank, der sich vor mir in seiner Diplomarbeit mit der Thematik der Dyonen auseinandersetzte, mich sowohl bei der Implementierung der verschiedenen Methoden unterstützte, als auch für meinen Vortrag während der DPG Frühjahrstagung 2011 und geduldig erklärte, wenn ich Fragen hatte. Ich möchte auch gleich den verbleibenden Mitgliedern der Kollaboration danken, Dr. Ernst-Michael Ilgenfritz und Dr. Falk Bruckmann, für die anregenden Diskussionen und hilfreichen Hinweise via E-Mail und während der zahlreichen Telefonkonferenzen.

Ebenso danke ich den verbleibenden Mitgliedern der Arbeitsgruppe, die immer Tipps hatten und ein offenes Ohr für Probleme aller Art. Nicht zuletzt danke ich speziell Marcus Petschlies für seine \LaTeX -Vorlage.

Privat gebührt großer Dank meinen Kommilitonen und Freunden, stellvertretend für viele weitere seien Christian, Marc und Bettina genannt, die immer seelische Unterstützung bereit hielten und mich gelegentlich daran erinnerten, dass es auch abseits der Universität Dinge gibt, die es wert sind, zu beschauen, wie z.B. die Quitte, der ich für den entspannten Urlaub kurz vor der Abgabe danken möchte.

Zuletzt spreche ich den größten Dank meiner geliebten Familie aus, meinen Eltern Berndt und Carola, meinem Stiefvater Ralf und meinen Brüdern Daniel und Rolf. Sie unterstützten mich bedingungslos auf jede erdenkliche Art und Weise und beschwerten sich nicht, wenn ich in der Versunkung verschwand, um zu lernen oder meine Arbeit zu schreiben.

Bei der Entstehung dieser Arbeit wurden keine Tiere verletzt (abgesehen von ein paar Mücken).

Selbständigkeitserklärung

Hiermit erkläre ich, die vorliegende Arbeit selbständig ohne fremde Hilfe verfasst und nur die angegebene Literatur und Hilfsmittel verwendet zu haben.

Berlin, 22. August 2011

Benjamin Frank Maier